

Contents lists available at ScienceDirect

Biochimica et Biophysica Acta

journal homepage: www.elsevier.com/locate/bbadis

Mitochondrial involvement and erythronic acid as a novel biomarker in transaldolase deficiency

Udo F.H. Engelke^{a,*}, Fokje S.M. Zijlstra^a, Fanny Mochel^b, Vassili Valayannopoulos^c, Daniel Rabier^c, Leo A.J. Kluijtmans^a, András Perl^d, Nanda M. Verhoeven-Duif^e, Pascale de Lonlay^f, Mirjam M.C. Wamelink^g, Cornelis Jakobs^g, Éva Morava^a, Ron A. Wevers^a

^a Radboud University Nijmegen Medical Centre, Department of Laboratory Medicine, Laboratory of Genetic Endocrine and Metabolic Diseases, Nijmegen, The Netherlands

^b Hôpital de La Salpêtrière, Department of Genetics and INSERM UMR S975, Paris, France

^c Hôpital Necker-Enfants Malades, Department of Metabolic Disorders, Paris, France

^d SUNY Upstate Medical University, Department of Medicine, Syracuse, NY, USA

^e University Medical Center Utrecht, Department of Metabolic and Endocrine Diseases, Utrecht, The Netherlands

^f Hôpital Necker, Centre de Référence des Maladies Héritaires du Métabolisme, Paris, France

^g VU University Medical Center, Department of Clinical Chemistry, Metabolic Unit, Amsterdam, The Netherlands

ARTICLE INFO

Article history:

Received 23 April 2010

Received in revised form 11 June 2010

Accepted 11 June 2010

Available online 18 June 2010

Keywords:

NMR spectroscopy

Citric acid cycle intermediates

Pentose phosphate pathway

Transaldolase deficiency

Polyols

Sedoheptulose

Erythronic acid

2-Oxoglutaric acid

ABSTRACT

Background: Sedoheptulose, arabitol, ribitol, and erythritol have been identified as key diagnostic metabolites in TALDO deficiency. **Method:** Urine from 6 TALDO-deficient patients and TALDO-deficient knock-out mice were analyzed using ¹H-NMR spectroscopy and GC–mass spectrometry. **Results:** Our data confirm the known metabolic characteristics in TALDO-deficient patients. The β-furanose form was the major sedoheptulose anomer in TALDO-deficient patients. Erythronic acid was identified as a major abnormal metabolite in all patients and in knock-out TALDO mice implicating an as yet unknown biochemical pathway in this disease. A putative sequence of enzymatic reactions leading to the formation of erythronic acid is presented. The urinary concentration of the citric acid cycle intermediates 2-oxoglutaric acid and fumaric acid was increased in the majority of TALDO-deficient patients but not in the knock-out mice. **Conclusion:** Erythronic acid is a novel and major hallmark in TALDO deficiency. The pathway leading to its production may play a role in healthy humans as well. In TALDO-deficient patients, there is an increased flux through this pathway. The finding of increased citric acid cycle intermediates hints toward a disturbed mitochondrial metabolism in TALDO deficiency.

© 2010 Elsevier B.V. All rights reserved.

1. Introduction

Two new defects in the pentose phosphate pathway (PPP) have recently been discovered: ribose 5-phosphate isomerase (RPI) deficiency (OMIM 608611) and transaldolase (TALDO) deficiency (OMIM 606003).

The first and as yet only case of RPI deficiency was described by Huck et al. [1]. The patient was a 14-year-old boy with leukoencephalopathy and peripheral neuropathy. Magnetic resonance spectroscopy (MRS) showed elevated levels of the polyols ribitol and

arabitol in the brain. Ten patients from six families with TALDO deficiency are known [2–5]. The disease is associated with liver symptoms, while other organs are affected to a variable degree [4,5]. The metabolic phenotype of this disease is characterized by increased urinary concentrations of the polyols erythritol, arabitol, ribitol, sedoheptitol, perseitol, the sugars sedoheptulose and mannoheptulose, and sedoheptulose-7-phosphate [4,6]. Erythritol, arabitol, and sedoheptulose have been described as most prominent diagnostic metabolites in urine of patients.

The biochemical diagnosis of RPI and TALDO deficiencies relies on finding strongly increased concentrations of polyols in body fluids. The use of LC–MS/MS, LC–MS, and GC–MS for this purpose has been reported [7–9]. ¹H-NMR spectroscopy can be used for identification and quantification of proton-containing metabolites in body fluids [10]. RPI deficiency was diagnosed successfully by measuring high concentrations of ribitol and arabitol in urine and cerebrospinal fluid (CSF) using NMR spectroscopy [11].

In this study, we had the opportunity to characterize urine from 6 patients with genetically confirmed TALDO deficiency. We show

Abbreviations: CSF, Cerebrospinal fluid; GC–MS, Gas chromatography–mass spectrometry; IEM, Inborn error of metabolism; LC–MS, Liquid chromatography–mass spectrometry; OMIM, Online Mendelian inheritance in man; PPP, Pentose phosphate pathway; RPI, Ribose 5-phosphate isomerase; TALDO, Transaldolase; TLC, Thin layer chromatography; TSP, Trimethylsilyl-2,2,3,3-tetradeuterium propionic acid

* Corresponding author. Radboud University Nijmegen Medical Centre, Department of Laboratory Medicine, Laboratory of Genetic Endocrine and Metabolic Diseases, Geert Grooteplein 10, 6525 GA Nijmegen, The Netherlands. Fax: +31 24 3668754.

E-mail address: u.engelke@labgk.umcn.nl (U.F.H. Engelke).

Table 1Concentrations ($\mu\text{mol}/\text{mmol}$ creatinine) of metabolites found in the urine from patients with TALDO deficiency.

Patient	Age ^a	Sedoheptulose ^b (β -furanose)	Erythronic acid ^b	Erythritol ^c	Ribitol ^c	Arabitol ^c	Oxoglutaric acid ^b	Fumaric acid ^b
1	16 y	390	550	137	67	142	130	42
2 ^d	1 m	1700	2900	1058	234	345	nd	20
3 ^d	4 y	160	770	205	41	192	50	44
4 ^e	3 y	290	350	217	167	253	280	8
5 ^e	1 y	870	670	494	208	298	440	8
6	4 y	350	350	290	137	262	1090	110
R	0–3 m	<40 [6]	<120	58–162 [9]	7–16 [9]	27–97 [9]		
R	1–2 y	<10 [6]	<50	76–192 [9]	9–24 [9]	52–88 [9]		
R	2–6 y	<10 [6]	<50	55–104 [9]	8–11 [9]	32–78 [9]		
R	18–80 y	<10 [6]	<50	19–76 [9]	2–5 [9]	10–44 [9]		
R	≤ 5 y						30–117 [20]	4–10 [20]
R	>5 y						2–95 [20]	nd–4 [20]

^ay, year(s), m, month(s); ^banalyzed by ¹H-NMR; ^canalyzed by GC-MS; ^{d,e}Sibs from 2 different families; R, Reference range; nd, not detectable.

for the first time the presence of increased urinary erythronic acid in all TALDO-deficient patients and show that this metabolite is a biochemical hallmark of TALDO deficiency. Furthermore, resonances of the β -furanose anomer of sedoheptulose were identified and quantified in all urine NMR spectra of the TALDO patients.

2. Materials and methods

2.1. Patients

Six patients from 4 families with TALDO deficiency were included in this study (Table 1). Clinical details about patients 1–3 have been described elsewhere (patient 1 [2], patients 2 and 3 [12]). In patients

4, 5, and 6, the diagnosis TALDO deficiency was confirmed at the metabolite level and the molecular genetic level.

2.2. Mice

Urine from TALDO-deficient “knock-out” mice was obtained from Dr. András Perl [7].

2.3. Authentic standards

Sedoheptulose is not commercially available and was isolated from the hybrid plant *Sedum spectabile* “Brillant” [13]. Leaves and stalk (70 g wet weight) were homogenized in 100 ml water and centrifuged through a 10-kD filter to remove proteins. Subsequently, the ultrafiltrate

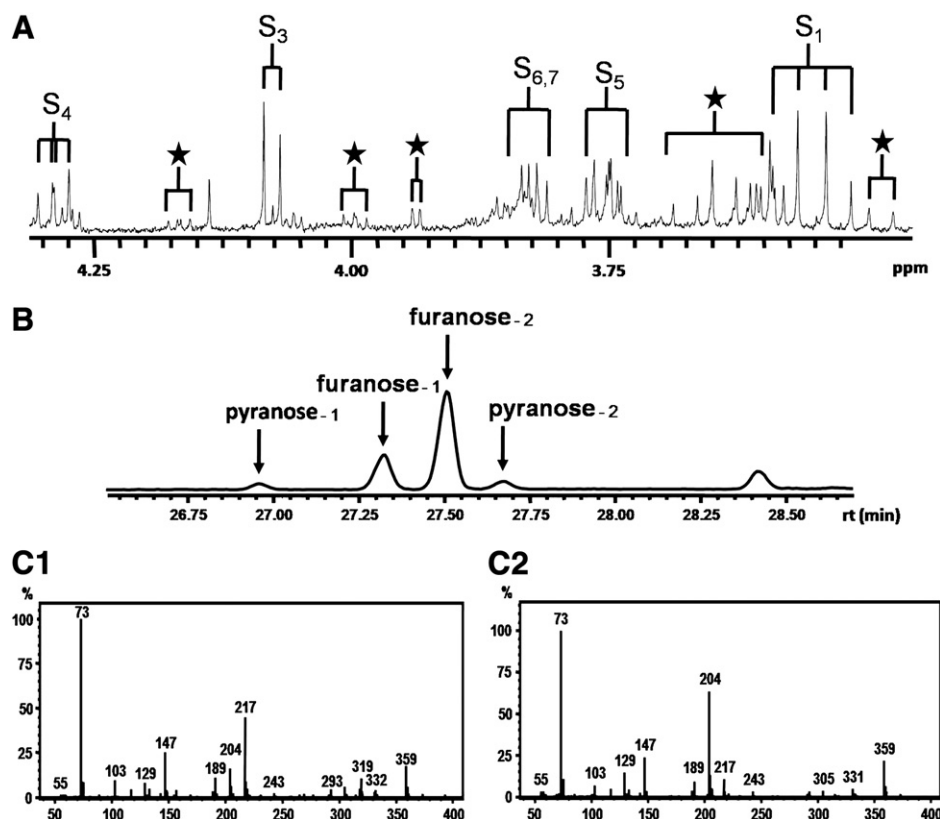


Fig. 1. Sedoheptulose purified from *Sedum spectabile* “Brillant”. (A) 500-MHz ¹H-NMR spectrum. Assignments “S” refer to the most prominent anomeric form of sedoheptulose, β -furanose. Subscript numbers refer to the carbon position in the molecule. Assignments “★” refer to the other anomeric forms of sedoheptulose. (B) GC profile: Pooled urine spiked with purified sedoheptulose. Sedoheptulose anomers were present in a ratio furanose-1/furanose-2/pyranose-1/pyranose-2 = 22%:64%:8%:6%. In all likelihoods, furanose-1 and pyranose-1 are alpha forms and furanose-2 and pyranose-2 are the beta forms. (C₁) Mass spectrum for the peak with assignment furanose-2 (m/z values {relative abundance}: 73(100), 217(45), 147(27), 204(18), and 359(15)). Characteristic for the furanose forms is the low ratio for m/z 204: m/z 217 [18]. (C₂) Mass spectrum for the peak with assignment pyranose-2 (m/z values {relative abundance}: 73(100), 204(62), 147(26), 359(22), and 217(12)). Characteristic for the pyranose forms is the high ratio for m/z 204: m/z 217 [18].

was concentrated by evaporation. The resulting preparation was further isolated preparatively by thin-layer chromatography (TLC) essentially as described by Engelke et al. [10] and measured as a model compound by $^1\text{H-NMR}$ spectroscopy and GC–MS (Fig. 1A and B, respectively).

Calcium L-threonic acid, potassium D-erythronic acid, and sedoheptulose-7-phosphate are commercially available from TCI Chemicals (Portland, USA), Carbosynth (Berkshire, UK), and Sigma-Aldrich (St. Louis, MO, USA), respectively.

2.4. Sample preparation

The urine samples were centrifuged before analysis. A volume of 70 μl of a 20.2 mmol/l trimethylsilyl-2,2,3,3-tetradeuteriumpropionic acid (TSP, sodium salt; Aldrich) $\cdot 2\text{H}_2\text{O}$ solution was added to 700 μl of urine as a chemical shift reference ($\delta = 0.00$) and as a lock signal. The pH of the urine was adjusted to 2.50 ± 0.05 with HCl. Finally, we placed 650 μl of the sample into a 5-mm NMR tube (Wilmad Royal Imperial; Wilmad LabGlass, USA).

2.5. One-dimensional $^1\text{H-NMR}$ spectroscopy and $^1\text{H-}^1\text{H}$ COSY spectroscopy

The urine samples were measured at 500 MHz on a Bruker DRX 500 spectrometer essentially as described before [14]. The samples were spun (14 Hz) during the 1D measurement. Shimming of the field

homogeneity was satisfactory when the TSP line width at half peak height was smaller than 1 Hz. Phasing of the spectra was completed manually, and the baseline was corrected using a cubic spline function. Metabolite resonances were fitted semi-automatically with a Lorentzian line shape and the resulting areas were compared with area of creatinine singlet (3.13 ppm; the N-CH₃ protons) to determine metabolite concentrations expressed as $\mu\text{mol}/\text{mmol}$ creatinine.

2.6. GC–mass spectroscopy

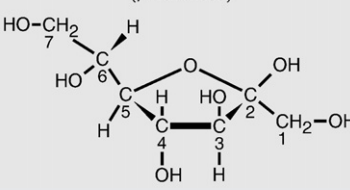
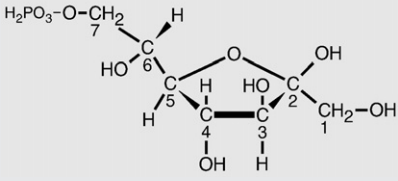
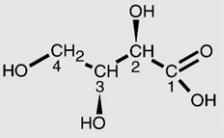
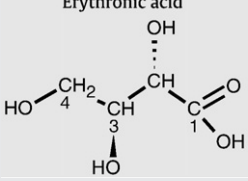
Monosaccharides and polyols were analyzed as trimethylsilyl derivatives by GC–MS essentially as described by Janssen et al. [9]. A VF-01 ms WCOT column (20 m \times 0.15 mm \times 0.15 μm) from Varian was used. The method is not optimally suited for quantification of sugar acids.

3. Results

3.1. Sedoheptulose

The $^1\text{H-NMR}$ spectrum of the isolated sedoheptulose in aqueous solution at pH 2.50 shows a complex pattern of resonances deriving from a mixture of furanose and pyranose anomers (Fig. 1A). Resonance assignments were based on previously reported NMR

Table 2
 $^1\text{H-NMR}$ assignments for sedoheptulose, sedoheptulose 7-phosphate, threonic acid, and erythronic acid.

Metabolite	Pos	Multiplicity*	Chemical shift (ppm)	
			pH 2.50	pH 7.00
 Sedoheptulose (β -furanose)	1	AB	3.55	3.58
	3	D	4.08	4.09
	4	DD	4.29	4.31
	5	M	3.75	3.77
	6, 7	Several	3.85–3.80	3.8
 Sedoheptulose 7-phosphate (β -furanose)	1	AB	3.56	3.54 [15]
	3	D	4.08	4.06 [15]
	4	DD	4.32	4.33 [15]
	5	M	3.81	3.78 [15]
	6, 7	Several	3.92	3.93 [15]
 Threonic acid	2	D	4.33	4.10
	3	M	4.07	3.98
	4	M	3.68	3.66
 Erythronic acid	2	D	4.32	4.10
	3	M	3.99	3.96
	4	M	3.69	3.66

Pos, carbon position in the molecule.

*D, doublet; M, multiplet; AB, AB system; DD, doublet–doublet.

spectra of sedoheptulose (The Human Metabolome Database (HMDB, <http://www.hmdb.ca>), HMDB ID 03219) and sedoheptulose-7-phosphate [15] and simulated NMR spectra of four sedoheptulose anomers: α -furanose, β -furanose, α -pyranose, and β -pyranose (ACD/HNMR Predictor, Advanced Chemistry Development, Toronto, Ontario, Canada). The $^1\text{H-NMR}$ spectrum shows that the β -furanose form of sedoheptulose had the highest concentration of the four anomeric forms. This is in line with observations on the anomeric forms of sedoheptulose-7-phosphate (α -furanose/ β -furanose/ α -pyranose = 20%:60%:20%) [15,16]. As indicated in Fig. 1A (★), the NMR spectrum showed smaller resonances at 4.17, 4.00, 3.94, 3.65, and 3.48 ppm representing the other anomeric forms of sedoheptulose. $^1\text{H-NMR}$ assignments for the β -furanose anomer of sedoheptulose are described in Table 2. The splitting pattern and order of shift are comparable with sedoheptulose-7-phosphate. GC-MS analysis showed the presence of four sedoheptulose anomers with the furanose anomer as the most prominent form (Fig. 1B). The furanose and pyranose anomers were identified by their characteristic m/z fragments (Fig. 1C₁ and C₂, respectively).

3.2. Sedoheptulose in urine

In Fig. 2D, the urine $^1\text{H-NMR}$ spectrum (4.4–3.4 ppm) from a 1-month-old TALDO patient is shown (Table 1, patient 2). Major metabolites in this region are creatinine (singlet at 4.29 ppm) and betaine (singlet at 3.97 ppm). Several unusual resonances were observed in this region (Fig. 2D, resonances S₁, S₃, S₄, E₂, E₃, and E₄). This pattern of resonances was found in the urine from all patients with TALDO deficiency and was not observed in NMR spectra of urine from 100 healthy children (age: 4 to 12 years). In TALDO deficiency,

high micromolar concentrations of sedoheptulose, erythritol, and arabitol are present in the urine [4]. Comparison of the urine from patient 2 with the spectrum of the isolated sedoheptulose shows that the unusual resonances S were caused by the β -furanose anomer of sedoheptulose (Fig. 2C and D). Confirmation was provided by a 2D COSY NMR experiment on the isolated sedoheptulose and the urine sample of TALDO patient 2. Two characteristic cross peaks of sedoheptulose with the coordinates 4.08/4.29 and 4.29/3.75 ppm were observed in the 2-dimensional NMR urine COSY spectra of the TALDO patients. Quantification of β -furanose sedoheptulose was performed on the doublet at 4.08 ppm (Fig. 2D, resonance S₃) and was 1700 $\mu\text{mol}/\text{mmol}$ creatinine in patient 2. In TALDO-deficient patients, the urinary concentration of β -furanose sedoheptulose ranged between 160 and 1700 $\mu\text{mol}/\text{mmol}$ creatinine (Table 1). The other three anomers of sedoheptulose (α -furanose, α -pyranose, and β -pyranose) were not observed in a urine NMR spectrum of the TALDO patients due to their low concentration and overlap by other resonances in the region between 4.3 and 3.5 ppm. The resonances of sedoheptulose-7P could not be observed in a 1D proton NMR spectrum of urine of our patients due to the known low concentration of sedoheptulose-7P in TALDO patients (2–24 $\mu\text{mol}/\text{mmol}$ creatinine) and overlap by other resonances [6].

GC-MS analysis confirmed the presence of abnormally high concentrations of sedoheptulose in the urine of all TALDO patients. The relative abundance of its four anomeric forms was similar for all TALDO urine samples and the sedoheptulose from *Sedum spectabile* (Fig. 1B). The mass spectrum shows a characteristic ratio for m/z 204 and 217 in the furanose and the pyranose anomers (Fig. 1C; [17,18]). The m/z 217 is caused by a strong ion $\text{RO-CH=CH-CH-O}^+\text{R}$ from furanoid hemiacetals while the m/z 204 derives from the $(\text{RO-CH-})_2^+$

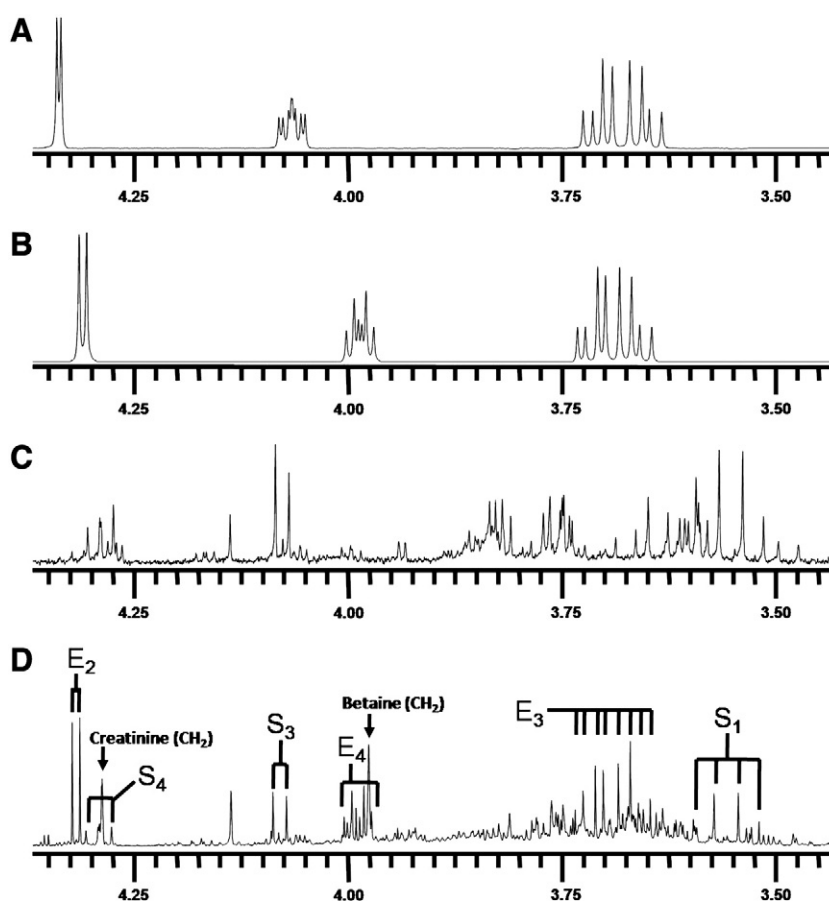


Fig. 2. *In vitro* $^1\text{H-NMR}$ spectra (500 MHz) of urine and model compounds measured at pH 2.50. (A) Threonic acid. (B) Erythronic acid. (C) Sedoheptulose isolated from *Sedum spectabile*. (D) Urine of a patient with transaldolase deficiency (S = sedoheptulose and E = erythronic acid. Subscript numbers refer to the carbon position in the molecule [Table 2]).

ion from pyranoid hemiacetals [18]. Comparison between the NMR data and the GC–MS profile makes it likely that the alpha forms of furanose and pyranose anomers have a shorter retention time on this column than the beta forms. In the GC–MS profile, the anomeric ratios of sedoheptulose were found to be furanose/pyranose = 86%:14% for urine of TALDO patients and 92%:8% for the sedoheptulose isolated from *Sedum spectabile*.

3.3. Erythritol, ribitol, and arabitol

GC–MS analysis of urine from TALDO patients shows elevated concentrations of erythritol, ribitol, and arabitol (Table 1). The resonances of these polyols could not be observed in either the 1D urine spectra or the 2D COSY NMR spectra. An explanation for this is that the protons of erythritol, ribitol, and arabitol have a high degree of splitting [11]. Identification and quantification of these polyols is further hampered by overlapping resonances from other urinary metabolites in the region 4.0–3.5 ppm [11].

3.4. Erythronic acid

The other unknown resonances in the 1D spectrum (Fig. 2D, resonances E₂, E₄, and E₃) could not be explained by the metabolite erythritol or arabitol. In order to identify resonances E, several NMR and GC–MS experiments were performed. COSY spectra revealed that the doublet resonance at 4.32 ppm was coupled with a resonance at 3.99 ppm. An NMR database (BRUKER, AMIX), containing spectra of 500 metabolites at various pH, revealed threonic acid as a candidate metabolite for the doublet resonance at 4.32 ppm. GC–MS analysis confirmed the presence of a high peak (with the same molecular

weight of threonic acid (MW = 136)) in urine samples of the TALDO patients. However, spiking threonic acid to the urine and 1D NMR experiments at various pH values proved that the resonances at 4.32 and 3.99 ppm were not caused by threonic acid.

Erythronic acid is the diastereomer of threonic acid. The compound is commercially available and was purchased at Carbosynth (Berkshire, UK). Erythronic acid in H₂O at pH 2.5 (Fig. 2B) showed resonances at 4.32 (doublet, $J=4.5$ Hz), 3.69 (multiplet), and 3.99 (multiplet) ppm (Table 2). Quantification of erythronic acid in urine samples was performed on the single proton attached to the C2 (Fig. 2D, resonance E₂) and the TSP singlet at 0.00 ppm was used as the concentration reference. After spiking erythronic acid to a urine sample at a level of 5.8 and 10.7 mmol/l, the recovery amounted to $\pm 90\%$.

Erythronic acid in H₂O at pH 2.5 (Fig. 2B) showed the same 1D and 2D resonance patterns as observed in the urine of the TALDO-deficient patients. The addition of pure erythronic acid to the urine sample of TALDO patient 5 resulted in an increase of the doublet at 4.32 ppm. Additionally, 1D ¹H-NMR spectra of erythronic acid and the urine sample were recorded at pH 7.0. Both spectra showed a doublet resonance that shifted from 4.32 ppm (pH 2.50) to 4.10 ppm (pH 7.0). These experiments confirmed the occurrence of erythronic acid in urine of TALDO-deficient patients. The erythronic acid concentration ranged between 350 and 2900 $\mu\text{mol}/\text{mmol}$ creatinine in the TALDO-deficient patients. In a control group of 100 healthy children (age: 4 to 12 years), we never found erythronic acid levels higher than 50 $\mu\text{mol}/\text{mmol}$ creatinine, in line with results reported by Guneal et al. [19]. In the urine from three newborns (age: 3 to 5 days), higher values up to 150 $\mu\text{mol}/\text{mmol}$ creatinine were found. Thus, erythronic acid occurs as a regular metabolite at low micromolar concentration in urine samples.

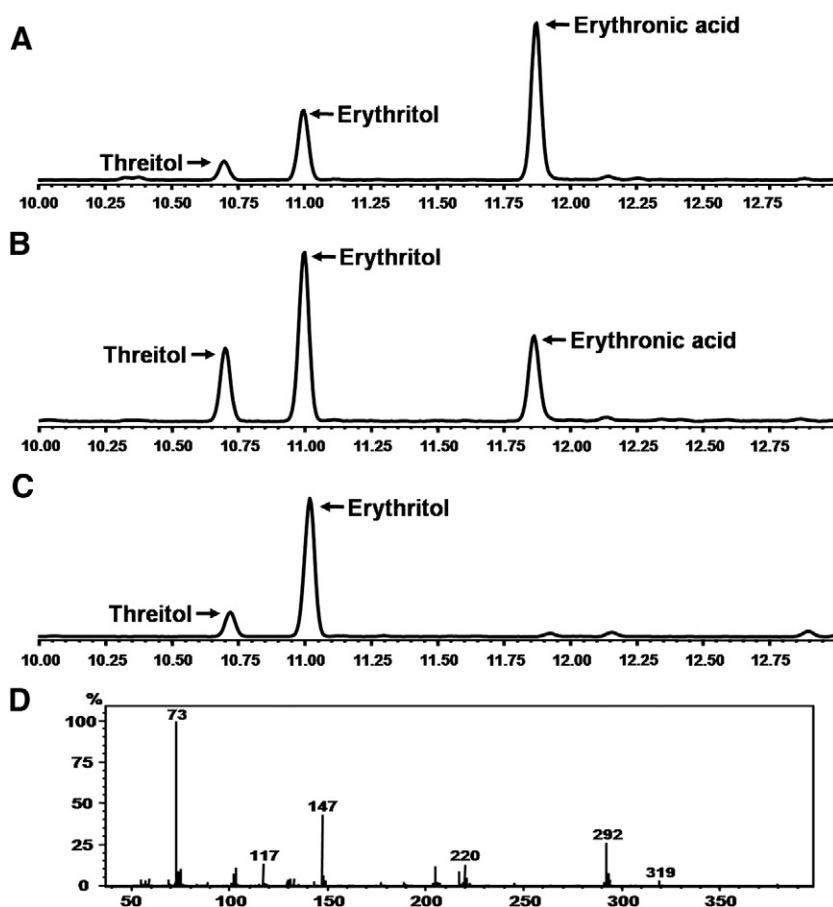


Fig. 3. GC–MS chromatogram of urine. (A) Pooled urine spiked with erythronic acid. (B) Urine of patient with transaldolase deficiency. (C) Control urine. (D) Mass spectrum of erythronic acid in the urine of the TALDO patient.

GC–MS analysis confirmed the presence of abnormally high concentrations of erythronic acid in the urine of TALDO patients. Fig. 3 shows the GC–MS chromatogram of a control urine (Fig. 3C) and urine from TALDO patient (Fig. 3B). The retention time and the mass spectrum of the erythronic acid peak in the urine of the TALDO patients correspond with the model compound spiked to a pooled urine sample (Fig. 3A).

3.5. Other metabolic abnormalities

In five out of six TALDO-deficient patients, the urinary concentration of 2-oxoglutaric acid was increased, varying between 50 and 1090 $\mu\text{mol}/\text{mmol}$ creatinine (reference ranges in $\mu\text{mol}/\text{mmol}$ creatinine: ≤ 5 years = 30–117, > 5 years = 2–95, adults = 4–74 [20]). 2-Oxoglutaric acid was not increased in urine samples from TALDO patient 2. Fumaric acid was increased in four of the six TALDO patients (patients 1, 2, 3, and 6; Table 1). The urine of patient 6 (4 years old) showed the highest concentration of 2-oxoglutaric acid (1090 $\mu\text{mol}/\text{mmol}$ creatinine) and fumaric acid (110 $\mu\text{mol}/\text{mmol}$ creatinine). The concentrations of other metabolites from the citric acid cycle, succinic acid and citric acid, were normal in all urine samples from the TALDO patients. In addition, lactate was normal in all TALDO urine samples and increased blood lactate has not been observed in these patients.

3.6. TALDO-deficient “knock-out” mice

The urine from two TALDO-deficient “knock-out” mice were measured by 1D and 2D ^1H -NMR spectroscopy and compared with the urine spectra from wild-type mice (Fig. 4). The 1D spectra of the two TALDO-deficient mice showed the presence of high concentrations of erythronic acid (1100 and 1700 $\mu\text{mol}/\text{mmol}$ creatinine) and of the β -furanose anomer of sedoheptulose (2300 and 3000 $\mu\text{mol}/\text{mmol}$ creatinine). These findings are consistent with the results observed in the urine NMR spectra of the TALDO-deficient patients.

The β -anomers of sedoheptulose and erythronic acid were not observed in the urine NMR spectra of the wild-type mice. 2-Oxoglutaric acid and fumaric acid had a normal concentration in the urine of TALDO-deficient and wild-type mice.

4. Discussion

^1H -NMR spectroscopy provides an overall view of proton-containing metabolites present in body fluids. Therefore, *in vitro* NMR spectroscopy is suited to diagnose patients with inborn errors of metabolism [10,21]. This study describes the *in vitro* NMR investigations at the metabolite level on 6 patients with TALDO deficiency. The 1D and 2D COSY ^1H -NMR spectra from these patients show a characteristic metabolic profile, mainly due to the resonances deriving from erythronic acid and the β -furanose anomer of sedoheptulose. GC–MS analysis confirmed the increased erythritol, ribitol, and arabitol concentrations in the urine from the TALDO-deficient patients. An increased concentration of erythronic acid in the urine of TALDO patients has not been described before. A low concentration of erythronic acid is always observed in urine from healthy children [19]. Our data show that on a molar basis, the excretion of erythronic acid is comparable to the sedoheptulose excretion. In this study, in 5 out of 6 TALDO-deficient patients, the concentration of erythronic acid in urine was higher than the concentration of the metabolites sedoheptulose, erythritol, ribitol, and arabitol. Therefore, erythronic acid ranks among the key metabolic features in TALDO deficiency and testifies a high flux through an as yet unknown metabolic pathway. As erythronic acid is always found in low concentration in the urine [19], the putative pathway shown in Fig. 5 may be present in healthy volunteers as well. The accumulation of erythronic acid in TALDO-deficient patients can putatively be explained as shown in Fig. 5. In TALDO deficiency, the flux through the PPP is disturbed leading to the accumulation of sedoheptulose-7-phosphate [4]. Wamelink et al. [4]

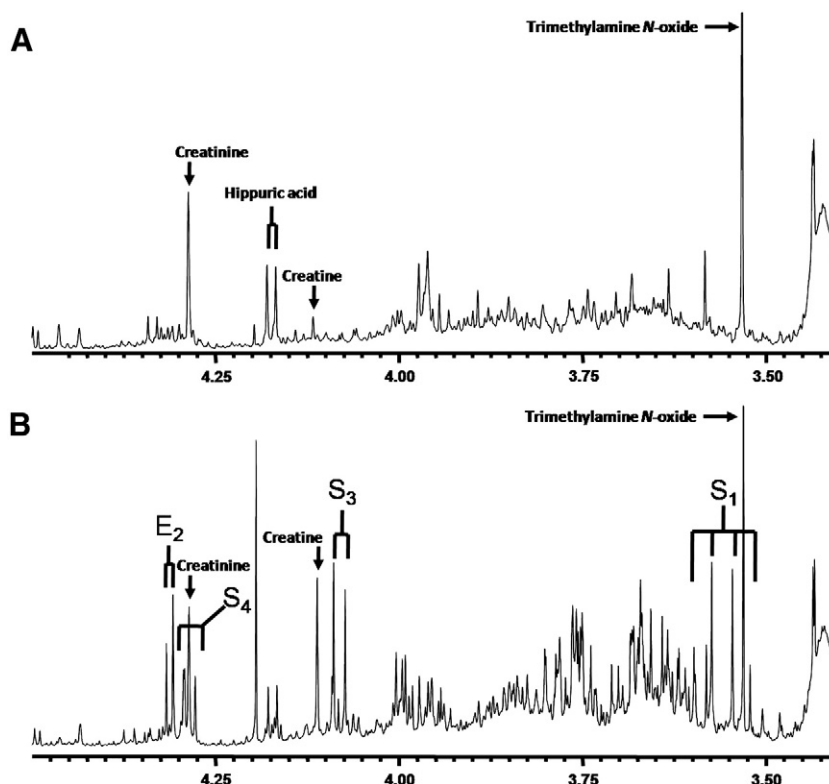


Fig. 4. *In vitro* ^1H -NMR spectra (500 MHz) of urine from mice measured at pH 2.50. (A) Urine of a control mouse. (B) Urine of a mouse with transaldolase deficiency (S = sedoheptulose and E = erythronic acid. Subscript numbers refer to the carbon position in the molecule [Table 2]).

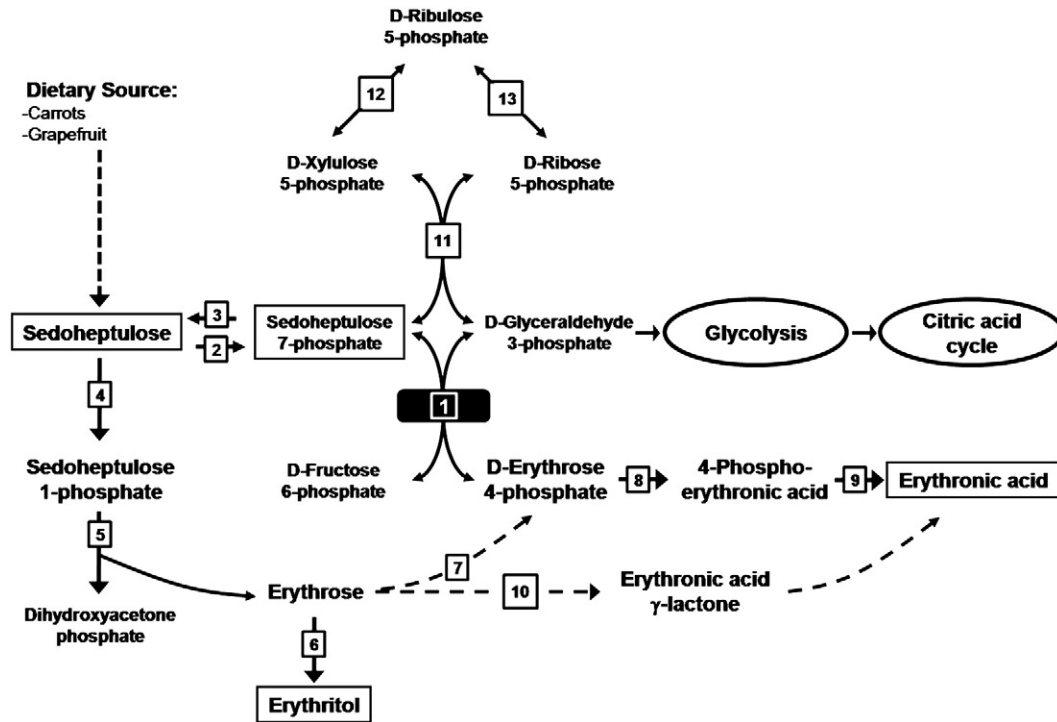


Fig. 5. Pentose phosphate pathway. Transaldolase deficiency (solid black square) results in accumulation of sedoheptulose, erythritol, and erythronic acid. (1) Transaldolase. (2) Sedoheptulokinase. (3) Cytosolic phosphatase. (4) Fructokinase. (5) Aldolase B. (6) Aldehyde reductase. (7) Putative (after Hauschildt et al. [23]). (8) Glyceraldehyde 3-phosphate dehydrogenase [24,25]. (9) Phosphatase. (10) Putative [26]. (11) Transketolase. (12) D-Ribulose 5-phosphate epimerase. (13) Ribose 5-phosphate isomerase.

speculated that the accumulation of sedoheptulose-7-phosphate is further metabolized into sedoheptulose as a detoxification process. Sedoheptulose can further be metabolized to erythrose via the enzymes fructokinase and aldolase (Fig. 5, enzymes 4 and 5 [22]). Subsequently, erythrose can be reduced to erythritol, which is found in high concentration in the urine of TALDO-deficient patients. Alternatively, erythrose may be phosphorylated into erythrose-4-phosphate as shown in Fig. 5, step 7 [23]. Erythrose-4-phosphate can be a substrate for transaldolase in some cell types. In addition, erythrose-4-phosphate is a known substrate for glyceraldehyde 3-phosphate dehydrogenase, converting it to 1,4-bis-phosphoerythronate or to 4-phosphoerythronate [24,25]. In patients with TALDO deficiency, the flux through this enzymatic reaction will increase. The next step in the formation of erythronic acid is most probably a dephosphorylation by one of the “non-specific” phosphatases that are present in all cells. Erythrose may also be converted to erythronic acid via lactone formation (Fig. 5, step 10) in a similar way as D-galactose can be converted in galactosemia patients via D-galactono-lactone to D-galactonic acid. Confirmation of the pathway leading to erythronic acid by further experiments is required [26]. The availability of TALDO knock-out mice is an advantage in this respect.

In almost all TALDO-deficient patients, urinary fumaric acid and 2-oxoglutaric acid were elevated while lactate and other metabolites from the citric acid cycle such as succinic acid and malic acid were normal. The mechanism behind this accumulation of specific citric acid cycle intermediates remains to be elucidated. Via D-glyceraldehyde 3-phosphate, an intermediate of the glycolysis, an increased flux through the glycolysis toward the citric acid cycle may occur in TALDO-deficient patients. However, this would only lead to accumulating citric acid cycle intermediates when there is uncoupling of the citric acid cycle and the respiratory chain or when there is direct inhibition of specific citric acid cycle enzymes. The observation of increased citric acid cycle intermediates is of potential clinical interest. As yet hyperlactacidemia has not been observed in TALDO deficiency and to our knowledge extensive testing of the respiratory

chain in muscle or liver of the patients has not been performed. Hanczko et al., however, did find evidence for mitochondrial dysfunction and oxidative stress in the liver of TALDO knock-out mice characterized by low NADPH, low glutathione, low ATP/ADP ratio, and accumulation of lipid hydroperoxides [27]. Our observations may be a starting point for further studies on mitochondrial aspects in human TALDO deficiency.

In conclusion, we have shown that NMR spectroscopy of urine can be used to diagnose patients with TALDO deficiency. The high urinary concentration of erythronic acid in TALDO patients has not been reported before and may serve as a new diagnostic hallmark of TALDO deficiency.

References

- [1] J.H. Huck, N.M. Verhoeven, E.A. Struys, G.S. Salomons, C. Jakobs, M.S. van der Knaap, Ribose-5-phosphate isomerase deficiency: new inborn error in the pentose phosphate pathway associated with a slowly progressive leukoencephalopathy, *Am. J. Hum. Genet.* 74 (2004) 745–751.
- [2] N.M. Verhoeven, J.H. Huck, B. Roos, E.A. Struys, G.S. Salomons, A.C. Douwes, M.S. van der Knaap, C. Jakobs, Transaldolase deficiency: liver cirrhosis associated with a new inborn error in the pentose phosphate pathway, *Am. J. Hum. Genet.* 68 (2001) 1086–1092.
- [3] N.M. Verhoeven, M. Wallot, J.H. Huck, O. Dirsch, A. Ballauf, U. Neudorf, G.S. Salomons, M.S. van der Knaap, T. Voit, C. Jakobs, A newborn with severe liver failure, cardiomyopathy and transaldolase deficiency, *J. Inherit. Metab. Dis.* 28 (2005) 169–179.
- [4] M.M. Wamelink, E.A. Struys, C. Jakobs, The biochemistry, metabolism and inherited defects of the pentose phosphate pathway: a review, *J. Inherit. Metab. Dis.* 31 (2008) 703–717.
- [5] A. Tylki-Szymanska, T.J. Stradomska, M.M. Wamelink, G.S. Salomons, J. Taybert, J. Pawlowska, C. Jakobs, Transaldolase deficiency in two new patients with a relative mild phenotype, *Mol. Genet. Metab.* 97 (2009) 15–17.
- [6] M.M. Wamelink, D.E. Smith, E.E. Jansen, N.M. Verhoeven, E.A. Struys, C. Jakobs, Detection of transaldolase deficiency by quantification of novel seven-carbon chain carbohydrate biomarkers in urine, *J. Inherit. Metab. Dis.* 30 (2007) 735–742.
- [7] G. Vas, K. Konkrite, W. Amidon, Y. Qian, K. Banki, A. Perl, Study of transaldolase deficiency in urine samples by capillary LC-MS/MS, *J. Mass Spectrom.* 41 (2006) 463–469.
- [8] M.M. Wamelink, D.E. Smith, C. Jakobs, N.M. Verhoeven, Analysis of polyols in urine by liquid chromatography–tandem mass spectrometry: a useful tool for

- recognition of inborn errors affecting polyol metabolism, *J. Inherit. Metab. Dis.* 28 (2005) 951–963.
- [9] G. Jansen, F.A. Muskiet, H. Schierbeek, R. Berger, W. van der Slik, Capillary gas chromatographic profiling of urinary, plasma and erythrocyte sugars and polyols as their trimethylsilyl derivatives, preceded by a simple and rapid prepurification method, *Clin. Chim. Acta* 157 (1986) 277–293.
- [10] U.F. Engelke, S.H. Moolenaar, S.M.G.C. Hoenderop, E. Morava, M. van der Graaf, A. Heerschap, R.A. Wevers, *Handbook of ¹H-NMR spectroscopy in inborn errors of metabolism: body fluid NMR spectroscopy and in vivo MR spectroscopy*, 2 ed. SPS Verlagsgesellschaft, Heilbronn, 2007.
- [11] S.H. Moolenaar, M.S. van der Knaap, U.F. Engelke, P.J. Pouwels, F.S. Janssen Zijlstra, N.M. Verhoeven, C. Jakobs, R.A. Wevers, In vivo and in vitro NMR spectroscopy reveal a putative novel inborn error involving polyol metabolism, *NMR Biomed.* 14 (2001) 167–176.
- [12] V. Valayannopoulos, N.M. Verhoeven, K. Mention, G.S. Salomons, D. Sommelet, M. Gonzales, G. Touati, P. de Lonlay, C. Jakobs, J.M. Saudubray, Transaldolase deficiency: a new cause of hydrops fetalis and neonatal multi-organ disease, *J. Pediatr.* 149 (2006) 713–717.
- [13] F.B. La Forge, C.S. Hudson, Sedoheptose, a new sugar from *Sedum spectabile*, *J. Biol. Chem.* 30 (1917) 61–77.
- [14] U.F. Engelke, B. Kremer, L.A. Kluijtmans, M. van der Graaf, E. Morava, F.J. Loupaty, R.J. Wanders, D. Moskau, S. Loss, E. van den Bergh, R.A. Wevers, NMR spectroscopic studies on the late onset form of 3-methylglutaconic aciduria type I and other defects in leucine metabolism, *NMR Biomed.* 19 (2006) 271–278.
- [15] F. Charmantray, V. Helaine, B. Legeret, L. Hecquet, Preparative scale enzymatic synthesis of D-sedoheptulose-7-phosphate from beta-hydroxypropyruvate and D-ribose-5-phosphate, *J. Mol. Catal. B Enzym.* 57 (2008) 6–9.
- [16] P.W. Kuchel, H.A. Berthon, W.A. Bubb, L.M. McIntyre, N.K. Nygh, D.R. Thorburn, ¹³C and ³¹P NMR studies of the pentose phosphate pathway in human erythrocytes, *Biomed. Biochim. Acta* 49 (1990) S105–S110.
- [17] A.C. Soria, M.L. Sanz, M. Villamiel, Determination of minor carbohydrates in carrot (*Daucus carota* L.) by GC–MS, *Anal. Methods* 114 (2009) 758–762.
- [18] Takuo Okuda, Setsuo Saito, Masayuki Hayashi, Trimethylsilylation and G.L.C.–mass spectrometry of 3-ketoses and 2-heptuloses, *Carbohydr. Res.* 68 (1997) 1–13.
- [19] F. Guneral, C. Bachmann, Age-related reference values for urinary organic acids in a healthy Turkish pediatric population, *Clin. Chem.* 40 (1994) 862–866.
- [20] N. Blau, M. Duran, M.E. Blaskovics, K.M. Gibson, *Physician's guide to the laboratory diagnostics of metabolic diseases*, 2 ed. Springer-Verlag, Berlin Heidelberg, 2003.
- [21] S.H. Moolenaar, U.F. Engelke, R.A. Wevers, Proton nuclear magnetic resonance spectroscopy of body fluids in the field of inborn errors of metabolism, *Ann. Clin. Biochem.* 40 (2003) 16–24.
- [22] T. Kardon, V. Stroobant, M. Veiga-da-Cunha, E.V. Schaftingen, Characterization of mammalian sedoheptulokinase and mechanism of formation of erythritol in sedoheptulokinase deficiency, *FEBS Lett.* 582 (2008) 3330–3334.
- [23] S. Hauschildt, R.A. Chalmers, A.M. Lawson, K. Schultis, R.W. Watts, Metabolic investigations after xylitol infusion in human subjects, *Am. J. Clin. Nutr.* 29 (1976) 258–273.
- [24] M.T. Ryzlak, R. Pietruszko, Heterogeneity of glyceraldehyde-3-phosphate dehydrogenase from human brain, *Biochim. Biophys. Acta* 954 (1988) 309–324.
- [25] Y. Ishii, T. Hashimoto, S. Minakami, H. Yoshikawa, The formation of erythronic acid 4-phosphate from erythrose 4-phosphate by glyceraldehyde-3-phosphate dehydrogenase, *J. Biochem.* 56 (1964) 111–112.
- [26] S.L. Wehrli, G.T. Berry, M. Palmieri, A. Mazur, L. Elsas, S. Segal, Urinary galactonate in patients with galactosemia: quantitation by nuclear magnetic resonance spectroscopy, *Pediatr. Res.* 42 (1997) 855–861.
- [27] R. Hanczko, D.R. Fernandez, E. Doherty, Y. Qian, G. Vas, B. Niland, T. Telarico, A. Garba, S. Banerjee, F.A. Middleton, D. Barrett, M. Barcza, K. Banki, S.K. Landas, A. Perl, Prevention of hepatocarcinogenesis and increased susceptibility to acetaminophen-induced liver failure in transaldolase-deficient mice by N-acetylcysteine, *J. Clin. Invest.* 119 (2009) 1546–1557.